

Supplementary materials

Effect of germanium incorporation on the electrochemical performance of electrospun Fe_2O_3 nanofibers-based anodes in sodium-ion batteries

Beatrix Petrovičovà¹, Chiara Ferrara^{2,3,*}, Gabriele Brugnetti², Clemens Ritter⁴, Martina Fracchia⁵, Paolo Ghigna⁵, Simone Pollastri⁶, Claudia Triolo^{1,3}, Lorenzo Spadaro⁷, Riccardo Ruffo^{2,3}, Saveria Santangelo^{1,3,*}

¹ Dipartimento di Ingegneria Civile, dell'Energia, dell'Ambiente e dei Materiali (DICEAM), Università Mediterranea di Reggio Calabria, 89122 Reggio Calabria, Italy; beatrice.petrovicova@unirc.it (B.P.); claudia.triolo@unirc.it (C.T.)

² Dipartimento di Scienza dei Materiali, Università di Milano Bicocca, 20125 Milano, Italy; g.brugnetti@campus.unimib.it (G.B.); riccardo.ruffo@unimib.it (R.R.)

³ National Reference Center for Electrochemical Energy Storage (GISEL) - Consorzio Interuniversitario Nazionale per la Scienza e Tecnologia dei Materiali (INSTM), 50121 Firenze, Italy

⁴ Institut Laue-Langevin - 71 avenue des Martyrs CS 20156, 38042 Grenoble, Cedex 9, France; ritter@ill.fr (C.R.)

⁵ Dipartimento di Chimica, Università degli studi di Pavia, 27100, Pavia, Italy; martina.fracchia02@universitadipavia.it (M.F.); paolo.ghigna@unipv.it (P.G.)

⁶ Elettra-Sincrotrone Trieste, 34149, Basovizza, Trieste, Italy; simone.pollastri@elettra.eu (S.P.)

⁷Istituto di Tecnologie Avanzate per l'Energia (ITAE) del Consiglio Nazionale delle Ricerche (CNR), 98126 Messina, Italy; lorenzo.spadaro@itaecnr.it (L.S.)

* Correspondence: chiara.ferrara@unimib.it (C.F.); saveria.santangelo@unirc.it (S.S.)

Preparation of the Electrospun NFs

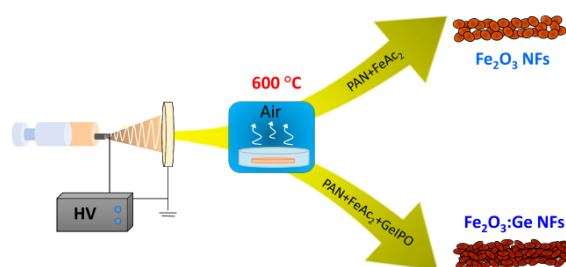


Figure S1. Sketch of the synthesis route followed to produce the electrospun iron oxide NFs.

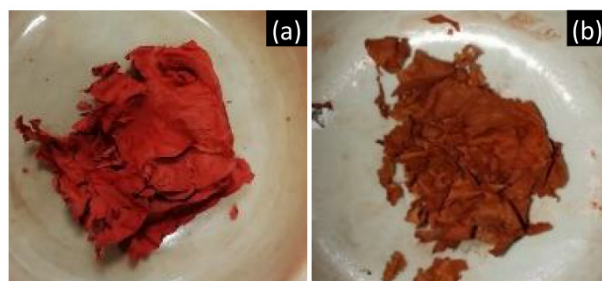


Figure S2. Photo of the as-calcined (a) Fe_2O_3 and (b) $\text{Fe}_2\text{O}_3:\text{Ge}$ NFs. The different colour hints at the formation of a different crystalline phase when germanium is incorporated.

Physicochemical Properties of the NFs

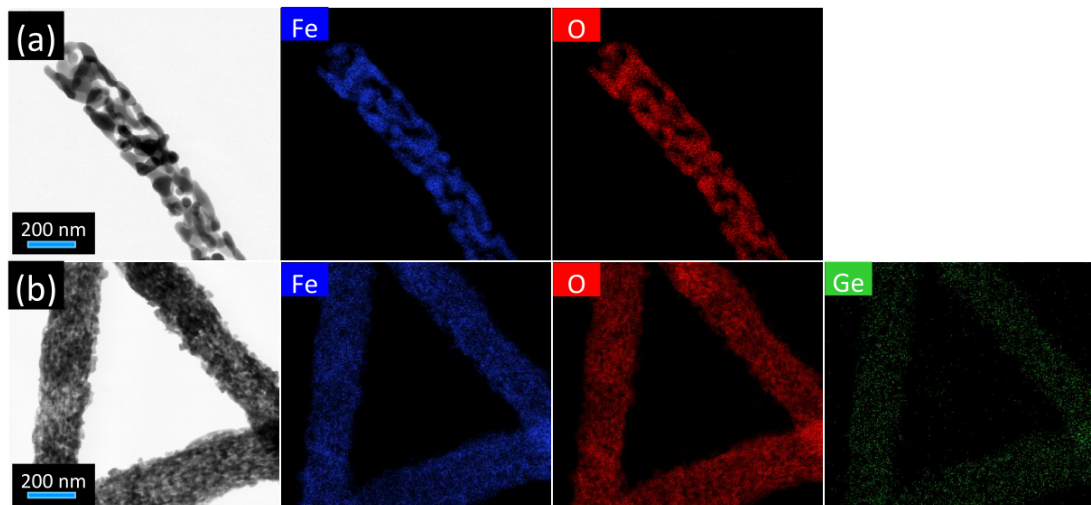


Figure S3. Elemental composition of the NFs (from HRTEM/EDX analysis). (a) Fe_2O_3 NFs and (b) $\text{Fe}_2\text{O}_3:\text{Ge}$ NFs.

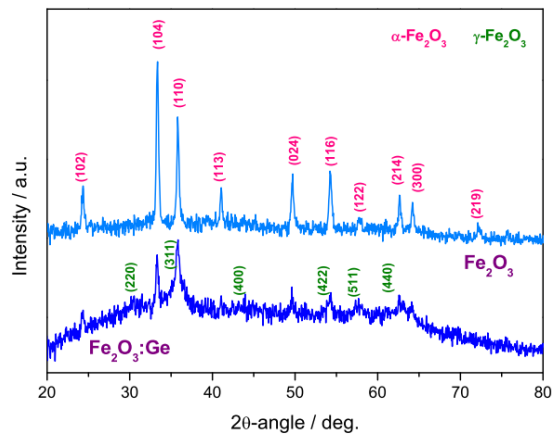


Figure S4. XRD patterns of the investigated NFs.

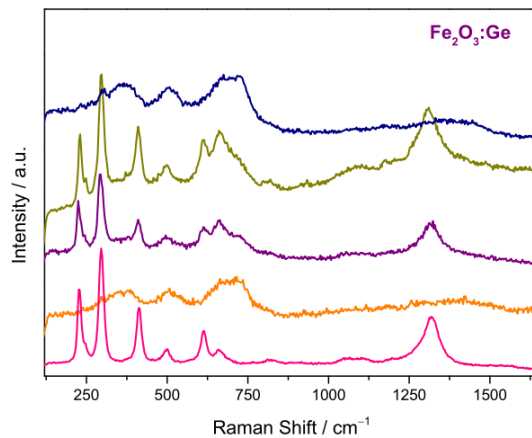


Figure S5. Micro-Raman spectra, as measured at different random locations in the sample. The incorporation of germanium reflected into a spatial inhomogeneity of the NFs, owing to the co-existence of α - and γ - polymorphs of the oxide.

Table S1. Surface composition of the NFs.

Sample	Fe / at%	O / at%	Ge / at%
Fe ₂ O ₃ NFs	30.4	69.6	0.0
Fe ₂ O ₃ :Ge NFs	20.2	68.8	11.0

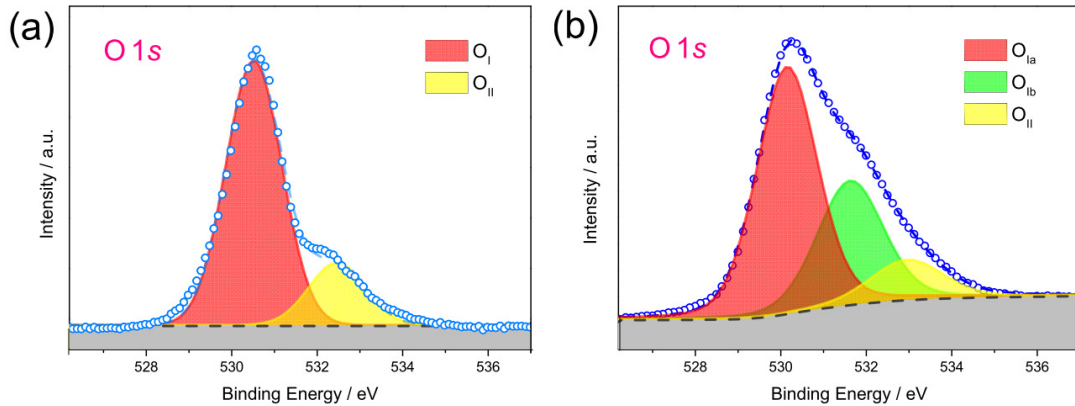


Figure S6. Deconvolution of the O 1s core level profiles of (a) Fe₂O₃ NFs and (b) Fe₂O₃:Ge NFs.

Table S2. Binding energies (in eV) and fractional area of the components of O 1s core level in the NFs.

Sample	O 1s					
	O _{Ia}		O _{Ib}		O _{II}	
	BE / eV	Area / %	BE / eV	Area / %	BE / eV	Area / %
Fe ₂ O ₃ NFs	530.54	83.2			532.41	16.8
Fe ₂ O ₃ :Ge NFs	530.15	57.6	531.64	31.4	532.66	11.1

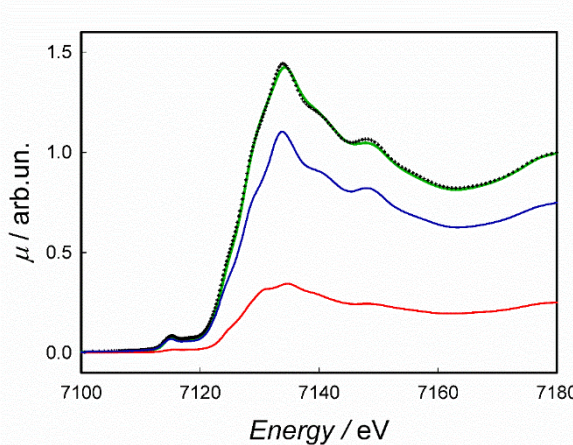


Figure S7. Linear combination fit of the spectrum of Fe₂O₃:Ge NFs acquired at the Fe K-edge. The green line represents the experimental signal, while the black dots represent the fit obtained with 77% of maghemite and

23% of hematite. The spectra of maghemite and hematite, weighed for 0.77 and 0.23, respectively, are shown as a blue and red line.

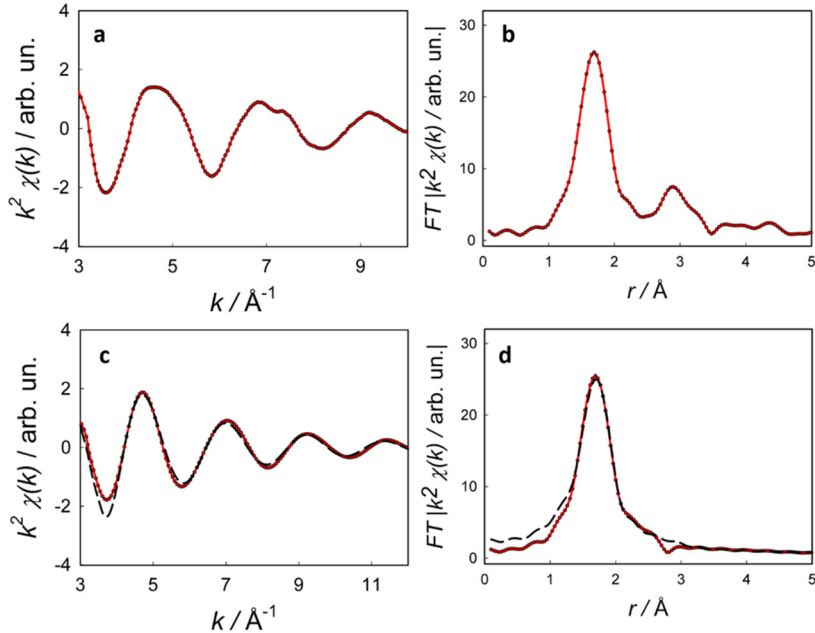


Figure S8. (a) EXAFS signal and (b) Fourier transform for the spectrum of $\text{Fe}_2\text{O}_3:\text{Ge}$ NFs at the Ge K-edge. The EXAFS and the Fourier transform after the Fourier filtering are shown in panel (c) and (d), respectively. The red line represents the experimental signal, while the black dotted line is the theoretical fit obtained starting from the GeO_4 structural model.

Table S3. Refined parameters obtained after the refinement of the Fourier-filtered signal. The goodness of fit (GOF), evaluated through the F factor ($F = 100 \sum_i^N \frac{(\chi_{i,\text{exp}} - \chi_{i,\text{calc}})^2}{\sigma_i}$), is 5.2%.

Shell	N	Atom	R(\AA)	σ^2 (\AA^2)
1	4	O	1.771(6)	0.0051(6)

Electrochemical Properties of the NFs

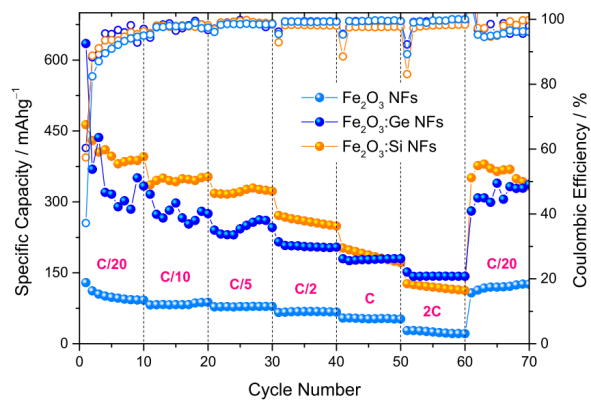


Figure S9. Results of the rate capability test on $\text{Fe}_2\text{O}_3:\text{Ge}$ NFs, compared with previously investigated Fe_2O_3 and $\text{Fe}_2\text{O}_3:\text{Si}$ NFs [S1].

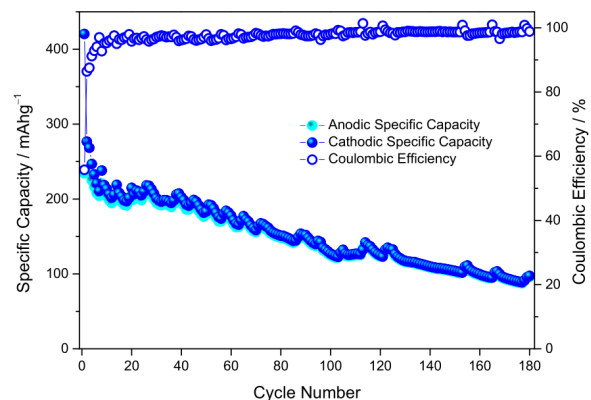


Figure S10. Results of the cyclability test on $\text{Fe}_2\text{O}_3:\text{Ge}$ NFs.

- S1. Fiore, M.; Longoni, G.; Santangelo, S.; Pantò, F.; Stelitano, S.; Frontera, P.; Antonucci, P.L.; Ruffo, R. Electrochemical characterization of highly abundant, low cost iron(III) oxide as anode material for sodium-ion rechargeable batteries. *Electrochim. Acta* **2018**, 269, 367–377.